Caveolin 1 Reduces High Glucose-Induced Hypertrophy and Inflammatory Fibrosis of H9C2 Cardiomyocytes By Inhibiting NF-κB Signaling

Wenyan Gong (yidagongwenyan@sina.com)
Hangzhou Normal University https://orcid.org/0000-0001-6950-7545

Jinghua Yuan
Hangzhou Normal University

Hui Luo
Hangzhou Normal University

Yingying Liu
Hangzhou No 2 People\'s Hospital: Hangzhou Normal University Affiliated Hospital

Mingwei Wang
Hangzhou No 2 People\'s Hospital: Hangzhou Normal University Affiliated Hospital

Xiaoling Xu
Hangzhou Normal University

Yusheng Cong
Hangzhou Normal University

Xingwei Zhang
Hangzhou Normal University

Original investigation

Keywords: Caveolin 1, DCM, cardiac hypertrophy, inflammatory fibrosis, NF-κB signaling

Posted Date: May 13th, 2021

DOI: https://doi.org/10.21203/rs.3.rs-507724/v1

Abstract

Background: Cardiac hypertrophy and inflammatory fibrosis are the basic pathological changes of the prevalent microvascular diabetes complication known as diabetic cardiomyopathy (DCM). Previous studies of the Caveolin 1 protein and the lipid raft structures known as caveolae—small invaginations of the plasma membranes of certain cell types (including cardiomyocytes)—have linked this protein to fat metabolism disorders, inflammation, diabetes, and cardiovascular disease. However, there are no reports linking Caveolin 1 to DCM. Here, we show that Caveolin 1 plays a vital role in the hypertrophy and inflammatory fibrosis of H9C2 cardiomyocytes induced by high glucose (HG) via inhibiting the NF-κB signaling.

Methods: The H9C2 cardiomyocytes induced by HG were used as the experimental model in this study to explicit the effect of Caveolin 1 on DCM and the underlying mechanisms involved. Unpaired Student's *t* test was used for comparison between two groups. For multiple comparisons, data were analyzed by one-way ANOVA with Bonferroni post hoc test multiple comparisons.

Results: (1) Exposure of H9C2 cardiomyocytes to HG activated NF-κB signaling and induced the expression of downstream NF-κB target genes including both hypertrophic factors and inflammatory fibrosis factors; (2) Intriguingly, exposure of cardiomyocytes to HG led to decreased Caveolin 1 levels, and this decrease occurred in an HG-exposure-time-dependent manner; (3) Overexpression of Caveolin 1 reduces phosphorylation of p65 and blocks the nuclear accumulation of this NF-κB component in HG-exposed cardiomyocytes, and inhibits transcriptional activation of NF-κB target genes; (4) Knocking down Caveolin 1 exacerbates the HG-induced promotion of the aforementioned NF-κB hypertrophic factors and inflammatory fibrosis factors, all of which have been linked to DCM pathogenesis.

Conclusions: Our study supports that Caveolin 1 can protect against hypertrophy and inflammatory fibrosis induced by HG, specifically by suppressing NF-κB signaling activity. Accordingly, some medical implications of our study include that i) Caveolin 1 may protect against the development of DCM and ii) may represent a target for developing therapeutics to protect against this highly prevalent and dangerous microvascular complications of diabetes.

Background

Cardiovascular disease (CVD) is the leading cause of death in people with type 2 diabetes mellitus (T2DM) [1]. Diabetic cardiomyopathy (DCM) is one of the major microvascular complications of diabetes that affects approximately 12% of diabetic patients, leading to overt heart failure and death [2]. The main pathologic changes of DCM include cardiac hypertrophy, myocardial fibrosis and ventricular dysfunction [3-5], which induce cardiac remodeling, cardiac dilatation, cardiac dysfunction and congestive heart failure, and eventually develop into heart failure, arrhythmia and cardiogenic shock [6-9].

Inflammation is an important feature of DCM [10-14]. Activation of the nuclear factor NF-κB lead to excessive expression of its down-stream target genes, such as inflammatory fibrosis components

including fibronectin (FN), intercellular adhesionmolecule-1 (ICAM-1), interleukin-6 (IL-6), monocyte chemoattractant protein-1 (MCP-1), tumor necrosis factor-α (TNF-α) and transforming growth factor-β1 (TGF-β1), and hypertrophic genes including atrial natriuretic facor (ANF) and brain natriuretic peptide (BNP), which promote the pathological process of cardiac hypertrophy and interstitial fibrosis of DCM [15, 16]. Therefore, inhibition of the expression of FN, ICAM-1, IL-6, MCP-1, TNF-α, TGF-β1, ANF and BNP induced by high glucose (HG) through NF-*κ*B signaling is beneficial to protect against DCM, and it is of great significance to explore the potential targets of anti-DCM which can inhibit the activation of NF-*κ*B inflammatory signaling.

Caveolin 1 is a major integral membrane protein in the cave-like invaginations on the cell surface (Caveolae). It participates in the regulation of a variety of cellular behaviors, including the formation and localization of Caveolae, maintenance of cellular cholesterol homeostasis and internalization of pathogens, and mediates maintaining the integrity of Caveolae and signal transduction [17-20]. Caveolin 1 knockout mice showed strong inflammatory responses and increased activation of NF-*κ*B and STAT3 pathways in the lungs, liver and kidneys [21], indicating Caveolin 1 regulates inflammatory response.

Recently, Caveolin 1 was found to play vital roles in diabetes and cardiovascular disease. In skeletal muscle biopsies of patients with type 2 diabetes, the expression of Caveolin 1 and eNOS were 50 percent lower than in normal tissue [22]. The Caveolin 1 levels decreased in mesenteric vascular smooth muscle cell from type 2 diabetic Goto-Kakizaki rats [23]. Besides, Caveolin 1 was also mediates β-cell apoptosis and proliferation [24], implying that Caveolin 1 may inhibit the development of diabetes. In the heart tissue of rat models of abdominal aortic constriction constructed left ventricular hypertrophy, the levels of Caveolin 1 decreased along with the increase of apelin receptor (APJ). Moreover, Caveolin 1 overexpression reduced the diameter and volume of H9C2 cells induced by Apelin-13 [25], demonstrating that Caveolin 1 alleviates the cardiac hypertrophy. All of these provided theoretical basis for Caveolin 1 as a potential target for the treatment of diabetes and cardiac hypertrophy.

Given the essential roles of Caveolin 1 in regulating the inflammation, diabetes and cardiac hypertrophy, our study aimed to elucidate the effects of Caveolin 1 on the HG-induced hypertrophy and inflammatory fibrosis of H9C2 cardiomyocytes, with special focus on the NF-*κ*B signaling pathway, which will contribute to serve Caveolin 1 as a new target for the study of DCM.

Materials And Methods

Reagents and antibodies

Dulbecco's modified Eagle's medium (DMEM) was purchased from Gibco Invitrogen Corporation (Gibco, Carlsbad, CA, USA). Polyvinylidene difluoride (PVDF) membranes were purchased from Immobilon®-PSQ (Millipore, CA, USA). An enhanced chemiluminescence substrate for the detection of Horseradish peroxidase (HRP) and a LightShift® chemiluminescent electrophoretic mobility shift assay (EMSA) kit were obtained from Thermo Fisher Scientific, Inc. (Rockford, USA). Biotin-labeled NF-*κ*B consensus

oligonucleotide, pNF-κB-luciferase plasmid and pRL-TK plasmid were acquired from Beyotime (Haimen, China). Antibodies against p65, Caveolin 1, FN, ICAM-1, IL-6 and MCP-1 (diluted 1: 500, Proteintech Group, Chicago, IL, USA), phosphorylation of p65, TGF-β1 (diluted 1: 1000) and β-actin (diluted 1: 5000, Cell Signaling Technology, Danvers, USA), Lamin B, ANF and BNP (diluted 1: 1000, Abcam, Cambridge, UK), TNF-α (diluted 1: 1000, Abclone, Baltimore Avenue, USA), rabbit IgG (Beyotime, Haimen, China) were purchased from commercial sources. HRP-conjugated secondary antibodies were acquired from Beyotime (Haimen, China).

Cell culture

Rat H9C2 cardiomyocytes were purchased from GuangZhou Jennio Biotech Co., Ltd (Jennio, Guangzhou, China). They were maintained in low glucose' DMEM in the presence of 10% fetal bovine serum (CellMax, Beijing, China) at 37 °C. Cells culture at 80% confluence were rendered quiescent by incubation for 12 h in serum-free medium before treating with HG' DMEM.

Plasmids, si-RNA, transient transfection

PcDNA3-Caveolin 1 was provided by Yusheng Cong (Institute of Aging Research, School of Medicine, Hangzhou Normal University); pcDNA3 vector was preserved in our laboratory. The si-RNA targeting *Caveolin 1* was purchased from GenePharma (GenePharma, shanghai, China). The special sequences of Caveolin 1-siRNA were displayed as: 5'-GACGUGGUCAAGAUUGACUTT-3', 3'-AGUCAAUCUUGACCACGUCTT-5'. We plated H9C2 cardiomyocytes in 60 mm plates 24 h prior to transfection. Dilute 5 μL Lipofectamine ® RNAiMAX Reagent in 125 μL Opti-MEM ® Medium, and dilute 5 μL siRNA in another 125 μL Opti-MEM ® Medium. Then add the diluted Caveolin 1 siRNA to diluted Lipofectamine ® RNAiMax Reagent (1: 1 ratio) and incubate 5 min. At last, the siRNA-reagent complex was added to H9C2 cells. After incubation 36 h, the transfection medium was abandoned and 2 mL low glucose' DMEM without serum was added to recover cell for 12 h. After specified treatment, the cells were collected for assays.

Western blot assays

Western blotting was carried out as previously described [26] to detect the protein levels of Caveolin 1, FN, ICAM-1, IL-6, MCP-1, TGF-β1, TNF-α, ANF, BNP phosphorylation and total NF-κB p65. The signals were visualized with a GE ImageQuant 350 instrument, and were quantified by densitometry using a Gel Doc XR System (Bio-Rad, USA); the signals were analyzed using Quantity One Protein Analysis Software (Bio-Rad).

Confocal laser scanning fluorescence microscopy

Immunofluorescence assay was carried out as previously described [27]. The images were collected using a DMi8 laser confocal fluorescence microscope (Nikon, Tokyo, Japan).

Nuclear protein extraction

The nuclear proteins were extracted with a Nuclear Extract Kit (BestBio, Shanghai, China). Cells were collected after centrifuging at 500 g for 3 minutes at 4 °C. PBS was used to wash the cells two times and the 200 μL cold Buffer A was added with 2μL protease inhibitor cocktail. Subsequently, the cells were vortexes with maximal velocity for 15 s and placed in the ice for 10 min. After being vortexes with maximal velocity for 5 s, the cells were centrifuged at 16,000g for 5 min at 4 °C and the supernatants (cytoplasm protein) were collected, besides, the sediments were added with 200 μL cold Buffer B with 2μL protease inhibitor cocktail. Afterwards, the sediments were vortexed with maximal velocity for 15 s and placed in the ice for 40 min. The supernatants (nuclear protein) were collected after centrifuged at 16,000g for 10 min at 4 °C.

Electrophoretic mobility shift assay (EMSA)

The EMSA assay was carried out as previously described [28]. Activation of NF-*κ*B signaling was determined based on EMSA using nuclear extracts, the sequence of the biotin-labeled oligonucleotide probes of nf-*κ*b was as follows: 5'-AGTTGAGGGGACTTTCCCAGGC-3', 3'-TCAACTCCCCTGAAAGGGTCCG -5' containing the acknowledged NF-*κ*B binding site. The procedures were performed following the instructions of the manufacturer (Light Shift Chemiluminescent EMSA Kit, Pierce, USA). The images were captured and quantified using Image Quant 350 (GE Healthcare, USA).

Dual luciferase reporter assay

The dual luciferase reporter assays were carried out as previously described [29]. H9C2 cardiomyocytes were seeded in 96-well culture plates and cotransfected with 0.1 μg of pNF-*κ*B -luciferase (Beyotime, Haimen, China) and 0.02 μg of pRL-TK (Beyotime, Haimen, China) in the presence or absence of 0.05 μg of Caveolin 1 plasmid or Caveolin 1 si-RNA. After various treatments, cells were lysed and the luciferase activity was determined using the Dual-Luciferase reporter assay system kit (Solarbio, Beijing, China) to analyze the effect of Caveolin 1 on the activation of NF-*κ*B pathway. Luciferase activity was normalized to the renilla luciferase activity.

Statistical analysis

Values were expressed as mean ± SEM. All data were assessed by the Graphpad Prism 5.0 software. Unpaired Student's *t* test was used for comparison between two groups. For multiple comparisons, data were analyzed by one-way ANOVA with Bonferroni post hoc test multiple comparisons. Independent experiments were performed at least thrice with similar results. $P < 0.05$ was considered statistically significant.

Results

HG induction causes hypertrophy and inflammatory fibrosis of H9C2 cardiomyocytes by activating NF-*κ*B signaling

NF-κB is a vital transcription factor that mediates inflammatory and its activation leads to cardiomyocyte injury in diabetes [30]. It consists of five members, including p65 (RelA), RelB, c-Rel, NF-κB1, and NF-κB2 [31]. HG is known to activate the NF-κB signaling in the H9C2 cardiomyocytes [32]. It was found that phosphorylation of the NF-κB p65 subunit and nuclear translocation of NF-κB p65 lead to the selective transcription of downstream proinflammatory genes [33, 34]. To verify the pathogenic impacts of HG on H9C2 cardiomyocytes, we detect the NF-κB signaling activation and accumulation of its down-stream target genes hypertrophic proteins (ANF and BNP) as well as inflammatory fibrosis factors (FN, ICAM-1, TGF-β1, IL-6, MCP-1 and TNF-α) levels.

Western blotting showed that the phosphorylation and nuclear accumulation of NF-κB p65 firstly up-regulated and then down-regulated with HG treatment compared to cells cultured in low glucose' DMEM, with a paramount up-regulation at 30 min, whereas total NF-κB p65 was not apparently changed (Fig. 1A-B). Meanwhile, the DNA-binding activity of NF-κB was measured by EMSA. The band intensity of the NF-κB-DNA oligonucleotide complex, which suggested the DNA-binding of NF-κB to its consensus DNA sequences was firstly increased and then decreased, with the maximal effect occurred after 30 min of HG treatment (Fig. 1C). Immunofluorescence results also showed that the cytoplasmic fluorescence of p65 dramatically attenuated, but the nuclear p65 significantly aggregated (Fig. 1D) after about 30 min incubation with HG. Besides, the ANF, BNP, FN, ICAM-1, TGF-β1, IL-6, MCP-1 and TNF-α levels significantly increased in the HG media experimental group compared to cells cultured in low glucose' DMEM, and these increases were in an exposure-time-dependent manner (Fig. 1E-G), indicating that our experimental cell model works and treatment with HG induces the hypertrophy and inflammatory fibrosis of H9C2 cardiomyocytes.

HG reduces Caveolin 1 levels in H9C2 cardiomyocytes

Previous study demonstrated that the Caveolin 1 expression decreased in skeletal muscle biopsies of patients with type 2 diabetes and the mesenteric vascular smooth muscle cells from type 2 diabetic rats [22, 23]. To investigate the effects of Caveolin 1 in HG-induction H9C2 cardiomyocytes, we performed western blotting to test whether HG affects the accumulation of Caveolin 1 firstly. Compared to cells cultured in low glucose media, the Caveolin 1 levels decreased dramatically in the HG media experimental group, with the extent of reduction increasing in an exposure-time-dependent manner (Fig. 2A), suggesting HG is a stimulator of Caveolin 1.

Caveolin 1 decreased the HG-induced accumulation of hypertrophic proteins and inflammatory fibrosis factors in H9C2 cardiomyocytes

We transfected with negative control (NC) and three pairs of siRNA oligonucleotides targeting *Caveolin 1* in H9C2 cardiomyocytes cultured with low glucose' DMEM. Preliminary testing showed that strongest interference effect was obtained for oligonucleotide pair 223 (Fig. 3A). We subsequently tested siRNA-mediated knockdown of *Caveolin 1* in HG-induction H9C2 cardiomyocytes and found that cells transfected with the *Caveolin 1* siRNA expressed lower overall Caveolin 1 levels than scramble control cells cultured in HG media (Fig. 3B), implying we successfully perform *Caveolin 1* knockdown.

Furthermore, we also transfected the hCaveolin 1 plasmids in HG-induction H9C2 cardiomyocytes to over expression Caveolin 1 (Fig. 3C).

Results in Fig.1 demonstrated that HG induces the hypertrophy and inflammatory fibrosis of H9C2 cardiomyocytes. Next, we knocked down *Caveolin 1* and transfected the hCaveolin 1 plasmids to detect the crucial role of Caveolin 1 in the hypertrophy and inflammatory fibrosis of H9C2 cardiomyocytes. Western blotting results showed that *Caveolin 1* knockdown led to increased accumulation of ANF, BNP, FN, ICAM-1, TGF-β1, IL-6, MCP-1 and TNF-α compared to scramble siRNA control HG culture cells (Fig. 4A-C). Moreover, overexpression of Caveolin 1 effectively inhibited HG induced up-regulation of ANF, BNP, FN, ICAM-1, TGF-β1, IL-6, MCP-1 and TNF-α compared to cells cultured in low glucose' DMEM (Fig. 4D-F).

Caveolin 1 knockdown activates NF-*κ*B signaling and enhances the DNA-binding and transcriptional activities of NF-*κ*B

Results above showed that the NF-*κ*B signaling was activated induced by HG. However, whether the role of Caveolin 1 in resisting the hypertrophy and inflammatory fibrosis of H9C2 cardiomyocytes related with the activation of NF-*κ*B signaling is unknown. To investigate the relationship between Caveolin 1 and the activation of NF-*κ*B signaling, we knocked down Caveolin 1 levels in HG-induction H9C2 cardiomyocytes and the activation of the NF-*κ*B signaling was detected.

It was shown that compared to cells cultured with low glucose' DMEM, *Caveolin 1* knockdown dramatically increased the HG-induced phosphorylation and nuclear distribution of NF-*κ*B p65, but decreased the cytoplasm distribution of p65 at 0.5 h (Fig. 5A-C). Meanwhile, the total expression of NF-*κ*B p65 had no significant change (Fig. 5A). Immunofluorescence analyses showed that after Caveolin 1 was knocked down, the HG-induced subcellular distribution of p65 in the nucleus was dramatically increased (Fig. 5D).

Moreover, EMSA and luciferase reporter assays results demonstrated that *Caveolin 1* knockdown further enhanced the HG-induced DNA-binding and transcriptional activities of NF-*κ*B (Fig. 5E-F).

Caveolin 1 overexpression inhibits NF-*κ*B signaling activation, and the DNA-binding and transcriptional activities of NF-*κ*B

To reconfirm the effects of Caveolin 1 on the activation of NF-*κ*B signaling, we transfected Caveolin 1 plasmids in H9C2 cells cultured with HG DMEM to detect the NF-*κ*B signaling activation.

Present results showed that compared with cells treated with low glucose' DMEM, overexpression of Caveolin 1 effectively suppressed the HG-induced phosphorylation and nuclear accumulation of NF-*κ*B p65 and enhanced p65 levels in the cytoplasm, whereas the total NF-*κ*B p65 levels were unchanged (Fig. 6A-C). Immunofluorescence analyses also revealed that the HG-induced subcellular distribution of p65 in the nucleus were obviously decreased by transfection with hCaveolin 1 plasmids (Fig. 6D), which was consistent with the western blot data.

Besides, to verify the effects of Caveolin 1 on the inhibition of HG-induced hypertrophy and inflammatory fibrosis of H9C2 cardiomyocytes were related with suppression the activation of NF-*κ*B signaling pathway, we conducted the EMSA and luciferase reporter assay to detect the roles of Caveolin 1 on the DNA-binding and transcriptional activities of NF-*κ*B. Results showed that overexpression of Caveolin 1 suppressed the HG-induced increase of the DNA-binding and transcriptional activities of NF-*κ*B compared to cells treated with low glucose' DMEM (Fig. 6E-F).

Collectively, these findings suggest that Caveolin 1 decreased the HG-induced accumulation of ANF, BNP, FN, ICAM-1, TGF-β1, IL-6, MCP-1 and TNF-α via inhibiting the NF-*κ*B signaling pathway.

Discussion

Cardiovascular complications, including DCM, account for significant morbidity and mortality in the diabetic population, and there is presently a lack of effective means to cure DCM [35]. Exploring new anti-DCM targets and therapeutic methods is therefore an urgent pursuit in DCM research. Multiple studies have used H9C2 cardiomyocytes exposed to HG for 24 h to induce an *in vitro* DCM model. HG treatment activates NF-*κ*B signaling [36, 37]. NF-*κ*B signaling activation triggers excessive and persistent expression of proinflammatory cytokines, including (among others) TNF-α, IL-6, and ICAM-1 [31, 38-42], as well as hypertrophic genes including ANF and BNP [43, 44]. These collectively exert numerous autocrine, pleiotropic effects in heart cells when exposed to various conditions, and can lead to ischemic myocardial injury, dilated cardiomyopathy, and HF, among other pathogenic phenotypes [45]. Moreover, it is known that activated NF-*κ*B signaling in the nucleus strongly induces TGF-β1 expression, which in turn up-regulates FN expression, resulting in excessive ECM in cardiac fibrosis [46].

In the present study, our results showed that both the phosphorylation and nuclear translocation of the NF-*κ*B signaling component p65 increased significantly in HG-stimulated H9C2 cardiomyocytes, whereas the total NF-*κ*B p65 levels remain unchanged. Moreover, treatment with HG for 24 h distinctly increased the accumulation of hypertrophic proteins (ANF and BNP) and inflammatory fibrosis factors (ICAM-1, TNF-α, IL-6, MCP-1, FN, and TGF-β1), collectively demonstrating that treatment with HG for 24 h induced inflammatory fibrosis and hypertrophy in H9C2 cardiomyocytes and establishing that NF-*κ*B signaling activation functionally contributes to this pathogenic process.

Caveolin 1, one of three known caveolin proteins (Caveolin 1, 2, and 3), occupies flask-shaped plasma membrane invaginations (also called caveolae) and serve as the structural components of caveolae [47]. Caveolin 1 is expressed ubiquitously in mammals as is caveolin 2, whereas Caveolin 3 is mostly found in skeletal muscle [47-49]. Previous studies have focused on correlations between Caveolin 3 and DCM [50, 51]. Induction of the caveolin-3/eNOS complex by nitroxyl (HNO) has been shown to ameliorate development of DCM [51]. However, it is still unknown whether Caveolin 1 or Caveolin 2 participates in mediating the pathological process of DCM. Notably, Caveolin 2 was shown to be coexpressed and to colocalize with Caveolin 1, and Caveolin 2 is known to require Caveolin 1 for proper membrane targeting

[52]. Moreover, Caveolin 3 is more similar to Caveolin 1 than to Caveolin 2 at the protein sequence level [53].

These previous observations motivated our interested in assessing the potential effects of Caveolin 1 in DCM and in exploring any underlying mechanisms. Briefly, our results showed that HG- decreased Caveolin 1 expression in H9C2 cardiomyocytes (in an exposure-time-dependent manner), indicating a potential link between down-regulation of Caveolin1 and the observed increases in inflammatory fibrosis factors like ICAM-1, TNF-α, IL-6, MCP-1, FN, and TGF-β1 as well as hypertrophic proteins like ANF and BNP. Furthermore, our study showed that overexpression of Caveolin 1 had an inhibitory effect on both HG-induced nuclear translocation of p65 and transcriptional activation of additional NF-*κ*B signaling components, while knocking down *Caveolin 1* exacerbated these HG-induced, DCM-linked pathogenic effects on H9C2 cardiomyocytes.

Accordingly, we infer that Caveolin 1 can somehow counteract the pathogenic impacts of HG on H9C2 cardiomyocytes through modulation of NF-*κ*B signaling activation. Elucidating the mechanisms through which Caveolin 1 regulates NF-*κ*B signaling will require further experimental work; at present, we hypothesize that Caveolin 1 may suppress the degradation of I*κ*B*α*, thereby blocking the release of NF-*κ*B dimers for translocation into the nucleus [54]. Given the known impact of the NEMO-containing IKK complex in promoting degradation of classical I*κ*Bs (I*κ*Bα, I*κ*Bβ, or I*κ*Bε) [55], it may be informative to explore potential interactions and impacts of Caveolin 1 with the kinase and/or regulatory subunits of the IKK complex.

Conclusions

In sum, our results showed that HG treatment decreased Caveolin 1 expression levels yet increased the nuclear translocation and transcriptional activation of NF-*κ*B signaling, which induced accumulation of inflammatory fibrosis factors FN, ICAM-1, TGF-β1, TNF-α, IL-6, MCP-1 and hypertrophic genes ANF and BNP in H9C2 cardiomyocytes. These HG-induced the effects on inflammatory fibrosis and hypertrophy in H9C2 cardiomyocytes were reversed upon overexpression of Caveolin 1 but were exacerbated by *Caveolin 1* knockdown in these HG-exposed cardiomyocytes. Considering that Caveolin 1 confers resistance against both inflammatory fibrosis and hypertrophy of H9C2 cardiomyocytes, our work supports the idea that Caveolin 1 may represent a potential therapeutic target for developing treatments for DCM.

Abbreviations

DCM: Diabetic Cardiomyopathy; HG: high glucose; FN: fibronectin; ICAM-1: intercellular adhesionmolecule-1; IL-6: interleukin-6; MCP-1: monocyte chemoattractant protein-1; TNF-α: tumor necrosis factor-α; TGF-β1: transforming growth factor-β1; ANF: atrial natriuretic facor; BNP: brain natriuretic peptide; HUVECs: human umbilical vein endothelial cells; APJ: apelin receptor; EMSA: electrophoretic mobility shift assay.

Declarations

Ethics approval and consent to participate

Not applicable.

Consent for publication

Not applicable.

Availability of data and materials

Data sharing is not applicable to this article as no datasets were generated or analysed during the current study.

Competing interests

The authors declare that they have no competing interests.

Fundings

This work was supported by research grants from the National Natural Science Foundation of China (No. 81900745), the Starting Foundation of Natural Science from Hangzhou Normal University (No. 2019QDL010), and the agricultural and social development research initiative design project of Hangzhou City (No. 20190101A03).

Authors' contributions

WYG designed and performed experiments, acquisition and analysis of data, and drafted the manuscript. JHY, HL, YYL and MWW helped to perform experiments and prepare the manuscript. XLX and YSC have been involved in drafting the manuscript and revising it critically for important intellectual content. XWZ and YSC contributed reagents/materials/analysis tools. All authors read and approved the final manuscript.

Acknowledgements

Not applicable.

References

1. Strain WD, Paldánius PM. Diabetes, cardiovascular disease and the microcirculation. Cardiovasc Diabetol. 2018;17(1):57.
2. Lorenzo-Almorós A, Tuñón J, Orejas M, Cortés M, Egido J, Lorenzo Ó. Diagnostic approaches for diabetic cardiomyopathy. Cardiovasc Diabetol. 2017;16(1):28.

3. Jia G, DeMarco VG, Sowers JR. Insulin resistance and hyperinsulinaemia in diabetic cardiomyopathy. Nat Rev Endocrinol. 2016;12(3):144–53.
4. Falcão-Pires I, Leite-Moreira AF. Diabetic cardiomyopathy: understanding the molecular and cellular basis to progress in diagnosis and treatment. Heart Fail Rev. 2012;17(3):325–44.
5. Fontes-Carvalho R, Ladeiras-Lopes R, Bettencourt P, Leite-Moreira A, Azevedo A. Diastolic dysfunction in the diabetic continuum: association with insulin resistance, metabolic syndrome and type 2 diabetes. Cardiovasc Diabetol. 2015;14:4.
6. Yang F, Qin Y, Lv J, Wang Y, Che H, Chen X, Jiang Y, Li A, Sun X, Yue E, Ren L, Li Y, Bai Y, Wang L. Silencing long non-coding RNA Kcnq1ot1 alleviates pyroptosis and fibrosis in diabetic cardiomyopathy. Cell Death Dis. 2018;9(10):1000.
7. Asbun J, Villarreal FJ. The pathogenesis of myocardial fibrosis in the setting of diabetic cardiomyopathy. J Am Coll Cardiol. 2006;47(4):693–700.
8. Devereux RB, Roman MJ, Paranicas M, O'Grady MJ, Lee ET, Welty TK, Fabsitz RR, Robbins D, Rhoades ER, Howard BV. Impact of diabetes on cardiac structure and function: the strong heart study. Circulation. 2000;101(19):2271–6.
9. Lee M, Gardin JM, Lynch JC, Smith VE, Tracy RP, Savage PJ, Szklo M, Ward BJ. Diabetes mellitus and echocardiographic left ventricular function in free-living elderly men and women: The Cardiovascular Health Study. Am Heart J. 1997;133(1):36–43.
10. Tschöpe C, Walther T, Escher F, Spillmann F, Du J, Altmann C, Schimke I, Bader M, Sanchez-Ferrer CF, Schultheiss HP, Noutsias M. Transgenic activation of the kallikrein–kinin system inhibits intramyocardial inflammation, endothelial dysfunction and oxidative stress in experimental diabetic cardiomyopathy. FASEB J. 2005;19(14):2057–9.
11. Lee TI, Kao YH, Chen YC, Huang JH, Hsiao FC, Chen YJ. Peroxisome proliferator-activated receptors modulate cardiac dysfunction in diabetic cardiomyopathy. Diabetes Res Clin Pract. 2013;100(3):330–9.
12. Westermann D, Linthout SV, Dhayat S, Dhayat N, Escher F, Bücker-Gärtner C, Spillmann F, Noutsias M, Riad A, Schultheiss HP, Tschöpe C. Cardioprotective and anti-inflammatory effects of interleukin converting enzyme inhibition in experimental diabetic cardiomyopathy. Diabetes. 2007;56(7):1834–41.
13. Zoubi SA, Chen J, Murphy C, Martin L, Chiazza F, Collotta D, Yaqoob MM, Collino M, Thiemermann C. Linagliptin Attenuates the Cardiac Dysfunction Associated With Experimental Sepsis in Mice With Pre-existing Type 2 Diabetes by Inhibiting NF-κB. Front Immunol. 2018;9:2996.
14. Li H, Shi Y, Wang X, Li P, Zhang S, Wu T, Yan Y, Zhan Y, Ren Y, Rong X, Xia T, Chu M, Wu R. Piceatannol alleviates inflammation and oxidative stress via modulation of the Nrf2/HO-1 and NF-κB pathways in diabetic cardiomyopathy. Chem Biol Interact. 2019;310:108754.
15. Nishikawa T, Edelstein D, Du XL, Yamaqishi S, Matsumura T, Kaneda Y, Yorek MA, Beebe D, Oates PJ, Hammes HP, Giardino I, Brownlee M. Normalizing mitochondrial superoxide production blocks three pathways of hyperglycaemic damage. Nature. 2000;404(6779):787–90.

16. Kim JA, Montagnani M, Koh KK, Quon MJ. Reciprocal relationships between insulin resistance and endothelial dysfunction: molecular and pathophysiological mechanisms. Circulation. 2006;113(15):1888–904.
17. Pelkmans L, Bürli T, Zerial M, Helenius A. Caveolin-stabilized membrane domains as multifunctional transport and sorting devices in endocytic membrane traffic. Cell. 2004;118(6):767–80.
18. Pelkmans L, Püntener D, Helenius A. Local actin polymerization and dynamin recruitment in SV40-induced internalization of caveolae. Science. 2002;296(5567):535–9.
19. Nichols BJ. A distinct class of endosome mediates clathrin-independent endocytosis to the Golgi complex. Nat Cell Biol. 2002;4(5):374–8.
20. Chun M, Liyanage UK, Lisanti MP, Lodish HF. Signal transduction of a G protein-coupled receptor in caveolae: colocalization of endothelin and its receptor with caveolin. Proc Natl Acad Sci USA. 1994;91(24):11728–32.
21. Yuan K, Huang C, Fox J, Gaid M, Weaver A, Li G, Singh BB, Gao H, Wu M. Elevated inflammatory response in caveolin-1-deficient mice with Pseudomonas aeruginosa infection is mediated by STAT3 protein and nuclear factor kappaB (NF-kappaB). J Biol Chem. 2011;286(24):21814–25.
22. Chen Z, Oliveira DS, Zimnicka S, Jiang AM, Sharma Y, Chen T, Lazarov S, Bonini O, Haus MG, Minshall JM. RD. Reciprocal regulation of eNOS and caveolin-1 functions in endothelial cells. Mol Biol Cell. 2018;29(10):1190–202.
23. Carrillo-Sepulveda MA, Matsumoto T. Phenotypic modulation of mesenteric vascular smooth muscle cells from type 2 diabetic rats is associated with decreased caveolin-1 expression. Cell Physiol Biochem. 2014;34(5):1497–506.
24. Li H, Peng H, Xu H, Xu F, Lin S, Lin K, Zeng W, Zeng L. The effects of caveolin 1 on β cell proliferation. Cell Mol Biol (Noisy-le-grand). 2018;64(1):40–6.
25. Wu D, Xie F, Xiao L, Feng F, Huang S, He L, Liu M, Zhou Q, Li L, Chen L. Caveolin-1-Autophagy Pathway Mediated Cardiomyocyte Hypertrophy Induced by Apelin-13. DNA Cell Biol. 2017;36(8):611–8.
26. Wang Y, Ye J, Li J, Chen C, Huang J, Liu P, Huang H. Polydatin ameliorates lipid and glucose metabolism in type 2 diabetes mellitus by downregulating proprotein convertase subtilisin/kexin type 9 (PCSK9). Cardiovasc Diabetol. 2016;15:19.
27. Gong W, Chen Z, Zou Y, Zhang L, Huang J, Liu P, Huang H. CKIP-1 affects the polyubiquitination of Nrf2 and Keap1 via mediating Smurf1 to resist HG-induced renal fibrosis in GMCs and diabetic mice kidneys. Free Radical Biol Med. 2018;115:338–50.
28. Gong W, Li J, Chen Z, Huang J, Chen Q, Cai W, Liu P, Huang H. Polydatin promotes Nrf2-ARE anti-oxidative pathway through activating CKIP-1 to resist HG-induced up-regulation of FN and ICAM-1 in GMCs and diabetic mice kidneys. Free Radic Biol Med. 2017;106:393–405.
29. Gong W, Chen C, Xiong F, Yang Z, Wang Y, Huang J, Liu P, Huang H. CKIP-1 ameliorates high glucose-induced expression of fibronectin and intercellular cell adhesion molecule-1 by activating the Nrf2/ARE pathway in glomerular mesangial cells. Biochem Pharmacol. 2016;116:140–52.

30. Frati G, Schirone L, Chimenti I, Yee D, Biondi-Zoccai G, Volpe M, Sciarretta S. An overview of the inflammatory signalling mechanisms in the myocardium underlying the development of diabetic cardiomyopathy. Cardiovasc Res. 2017;113(4):378–88.
31. Jimi E, Takakura N, Hiura F, Nakamura I, Hirata-Tsuchiya S. The Role of NF-κB in Physiological Bone Development and Inflammatory Bone Diseases: Is NF-κB Inhibition "Killing Two Birds with One Stone"? Cells. 2019;8(12):1636.
32. Pan Y, Wang Y, Zhao YJ, Peng KS, Li WX, Wang YG, Zhang JJ, Zhou SS, Liu Q, Li XK, Cai L, Liang G. Inhibition of JNK phosphorylation by a novel curcumin analog prevents high glucose-induced inflammation and apoptosis in cardiomyocytes and the development of diabetic cardiomyopathy. Diabetes. 2014;63(10):3497–511.
33. Shi H, Berger EA. Characterization of Site-Specific Phosphorylation of NF-κB p65 in Retinal Cells in Response to High Glucose and Cytokine Polarization. Mediators Inflamm. 2018; 2018: 3020675.
34. Zhang Q, Lenardo MJ, Baltimore D. 30 Years of NF-κB: A Blossoming of Relevance to Human Pathobiology. Cell. 2017;168(1–2):37–57.
35. Parim B, Uddandrao VVS, Saravanan G. Diabetic cardiomyopathy: molecular mechanisms, detrimental effects of conventional treatment, and beneficial effects of natural therapy. Heart Fail Rev. 2019;24(2):279–99.
36. Al-Malki WH, Abdel-Raheem IT. Cardioprotective effect of 6-shogaol against hyperglycemia-induced toxicity in H9c2 cardiomyocytes via suppressing of NF-κB pathway. Pak J Pharm Sci. 2019;32(1):327–31.
37. Huang Z, Dong X, Zhuang X, Hu X, Wang L, Liao X. Exogenous hydrogen sulfide protects against high glucose-induced inflammation and cytotoxicity in H9c2 cardiac cells. Mol Med Rep. 2016;14(5):4911–7.
38. Goebeler M, Gillitzer R, Kilian K, Utzel K, Bröcker EB, Rapp UR, Ludwig S. Multiple signaling pathways regulate NF-kappaB-dependent transcription of the monocyte chemoattractant protein-1 gene in primary endothelial cells. Blood. 2001;97(1):46–55.
39. Westermann D, Linthout SV, Dhayat S, Dhayat N, Escher F, Bücker-Gärtner C, Spillmann F, Noutsias M, Riad A, Schultheiss HP, Tschöpe C. Cardioprotective and anti-inflammatory effects of interleukin converting enzyme inhibition in experimental diabetic cardiomyopathy. Diabetes. 2007;56(7):1834–41.
40. Brasier AR. The nuclear factor-kappaB-interleukin-6 signalling pathway mediating vascular inflammation. Cardiovasc Res. 2010;86(2):211–8.
41. Steiner A, Harapas CR, Masters SL, Davidson S. An Update on Autoinflammatory Diseases: Relopathies. Curr Rheumatol Rep. 2018;20(7):39.
42. Rajesh M, Bátkai S, Kechrid M, Mukhopadhyay P, Lee WS, Horváth B, Holovac E, Cinar R, Liaudet L, Mackie K, Haskó G, Pacher P. Cannabinoid 1 receptor promotes cardiac dysfunction, oxidative stress, inflammation, and fibrosis in diabetic cardiomyopathy. Diabetes. 2012;61(3):716–27.

43. Ma KK, Banas K, Bold AJ. Determinants of inducible brain natriuretic peptide promoter activity. Regul Pept. 2005;128(3):169–76.
44. Gao H, Liu H, Tang T, Huang X, Wang D, Li Y, Huang P, Peng Y. Oleanonic acid ameliorates pressure overload-induced cardiac hypertrophy in rats: The role of PKCζ-NF-κB pathway. Mol Cell Endocrinol. 2018;470:259–68.
45. Turner NA, Mughal RS, Warburton P, O'Regan DJ, Ball SG, Porter KE. Mechanism of TNFalpha-induced IL-1alpha, IL-1beta and IL-6 expression in human cardiac fibroblasts: effects of statins and thiazolidinediones. Cardiovasc Res. 2007;76(1):81–90.
46. Chen S, Khan ZA, Cukiernik M, Chakrabarti S. Differential activation of NF-κB and AP-1 in increased fibronectin synthesis in target organs of diabetic complications. Am J Physiol Endocrinol Metab. 2003;284(6):E1089–97.
47. Krieken RV, Krepinsky JC. Caveolin-1 in the Pathogenesis of Diabetic Nephropathy: Potential Therapeutic Target? Curr Diab Rep. 2017;17(3):19.
48. Parton RG, Simons K. The multiple faces of caveolae. Nat Rev Mol Cell Biol. 2007;8(3):185–94.
49. Cohen AW, Hnasko R, Schubert W, Lisanti MP. Role of caveolae and caveolins in health and disease. Physiol Rev. 2004;84(4):1341–79.
50. Murfitt L, Whiteley G, Iqbal MM, Kitmitto A. Targeting caveolin-3 for the treatment of diabetic cardiomyopathy. Pharmacol Ther. 2015;151:50–71.
51. Sun HJ, Xiong SP, Wu ZY, Cao L, Zhu MY, Moore PK, Bian JS. Induction of caveolin-3/eNOS complex by nitroxyl (HNO) ameliorates diabetic cardiomyopathy. Redox Biol. 2020;32:101493.
52. Parolini I, Sargiacomo M, Galbiati F, Rizzo G, Grignani F, Engelman JA, Okamoto T, Ikezu T, Scherer PE, Mora R, Rodriguez-Boulan E, Peschle C, Lisanti MP. Expression of caveolin-1 is required for the transport of caveolin-2 to the plasma membrane. Retention of caveolin-2 at the level of the golgi complex. J Biol Chem. 1999;274(36):25718–25.
53. Tang Z, Scherer PE, Okamoto T, Song K, Chu C, Kohtz DS, Nishimoto I, Lodish HF, Lisanti MP. Molecular cloning of caveolin-3, a novel member of the caveolin gene family expressed predominantly in muscle. J Biol Chem. 1996;271(4):2255–61.
54. Sanchez AP, Sharma K. Transcription factors in the pathogenesis of diabetic nephropathy. Expert Rev Mol Med. 2009;11:e13.
55. Hayden MS, Ghosh S. Shared principles in NF-kappaB signaling. Cell. 2008;132(3):344–62.

Figures

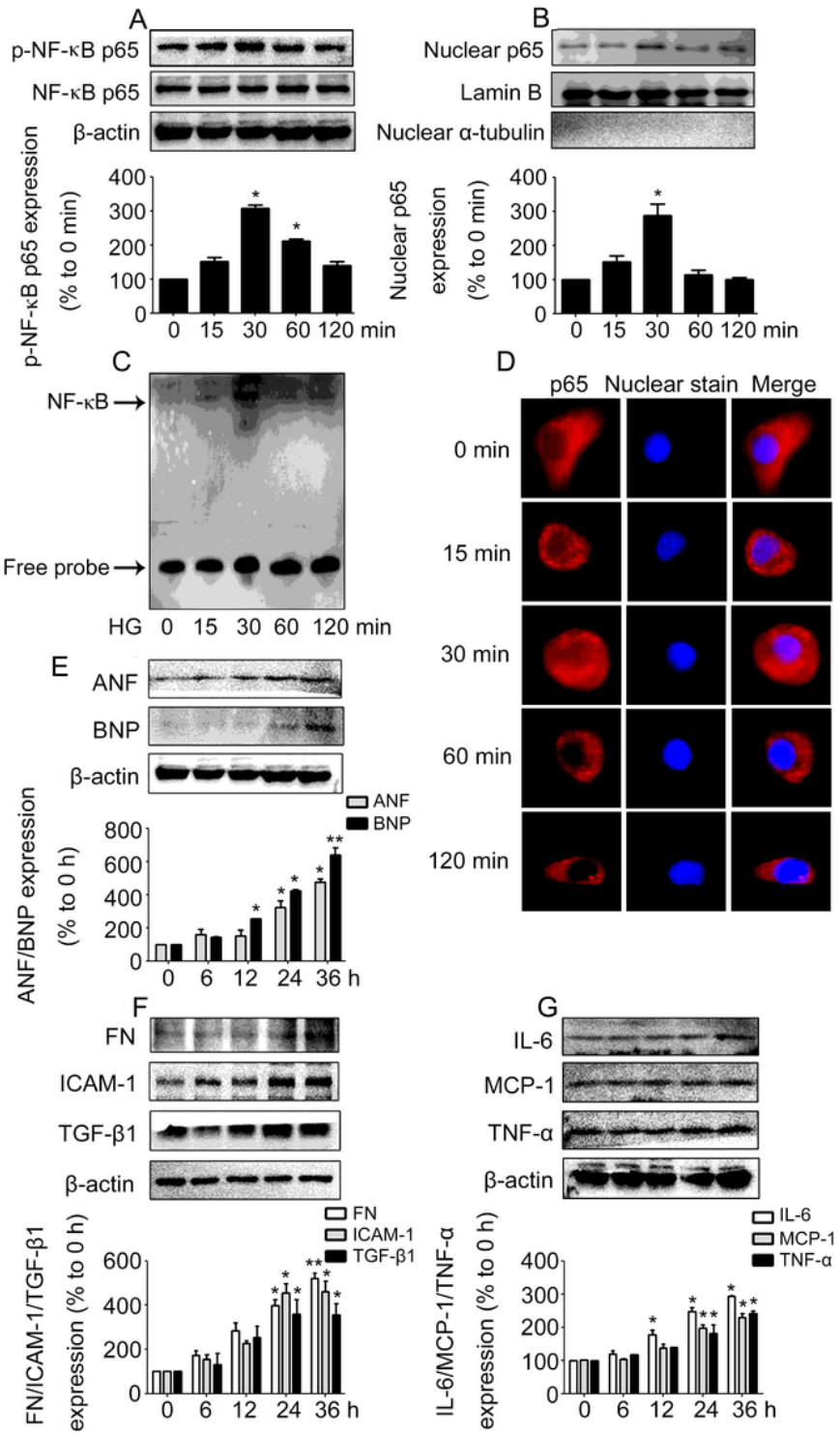

Figure 1

HG induction causes hypertrophy and inflammatory fibrosis of H9C2 cardiomyocytes by activating NF-κB signaling. The effects of HG on the phosphorylation and total accumulation of NF-κB p65 (A) and on nuclear accumulation of p65 (B) at the indicated time points assessed by western blotting. *P □ 0.05 vs 0 min. (C) EMSA was performed to investigate the DNA-binding activity of NF-κB. (D) Immunofluorescence staining for the subcellular distribution of p65 at the indicated time points in H9C2 cardiomyocytes

exposed to HG. Original magnification, ×630. The accumulation of ANF and BNP (E), FN, ICAM-1 and TGF-β1 (F), IL-6, MCP-1 and TNF-α (G), measured by western blotting of HG-exposed H9C2 cardiomyocytes at the indicated time points. *P □ 0.05, **P □ 0.01. All experiments were conducted at least three times and similar results were obtained each time.

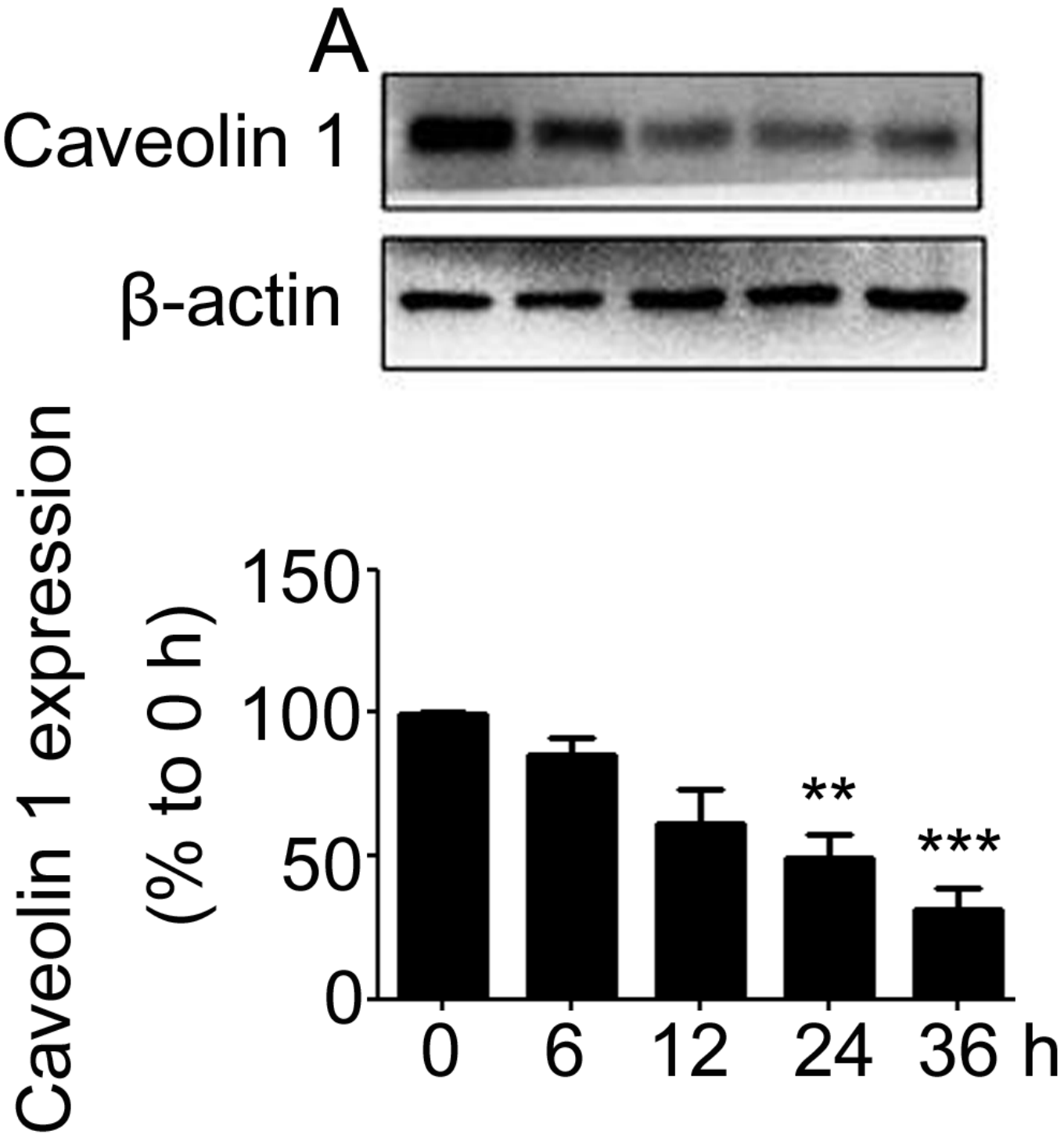

Figure 2

HG reduces Caveolin 1 levels in H9C2 cardiomyocytes. The Caveolin 1 levels (A) were detected by western blotting of HG-exposed H9C2 cardiomyocytes at the indicated time points. **P □ 0.01, ***P □ 0.001 vs 0 h.

This experiment was performed at least three times, with similar results obtain each time.

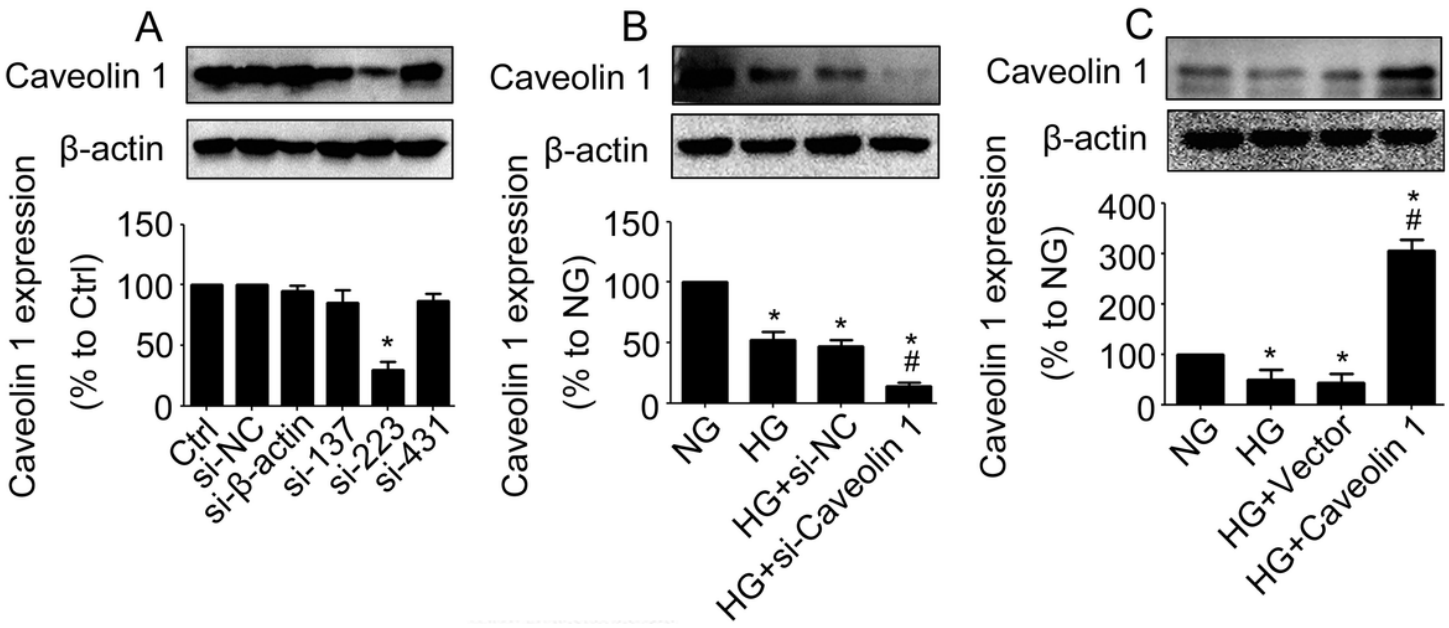

Figure 3

Caveolin 1 knockdown and overexpression. (A) Total protein was collected when cells were transfected with negative control (NC) or three pairs of siRNA oligonucleotides targeting Caveolin 1 (75 nM) for 72 h, followed by western blotting. *P < 0.05 vs Ctrl. The accumulation of Caveolin 1 was determined in the Caveolin 1 knockdown (B) and Caveolin 1 overexpression (C) HG-exposed H9C2 cardiomyocytes. *P < 0.05 vs NG, #P < 0.05 vs HG. All experiments were implemented at least three times with similar results.

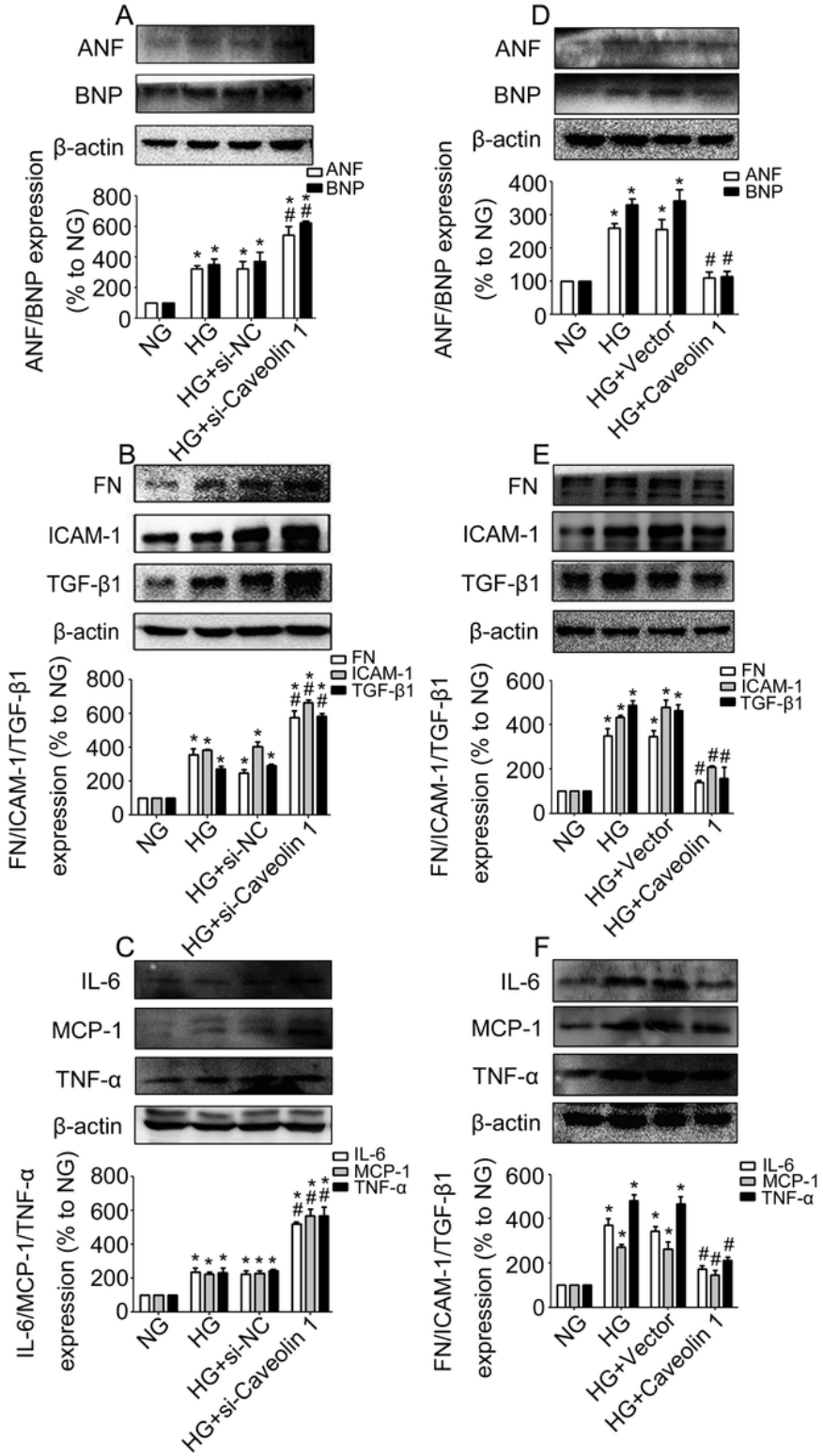

Figure 4

Caveolin 1 decreased the HG-induced accumulation of hypertrophic proteins and inflammatory fibrosis factors in H9C2 cardiomyocytes. ANF and BNP (A and D), FN, ICAM-1 and TGF-β1 (B and E), IL-6, MCP-1 and TNF-α levels (C and F), measured by western blotting of HG-exposed Caveolin 1 knockdown or overexpression H9C2 cardiomyocytes. *P < 0.05 vs NG, #P < 0.05 vs HG. This experiment was performed at least three times, with similar results obtain each time.

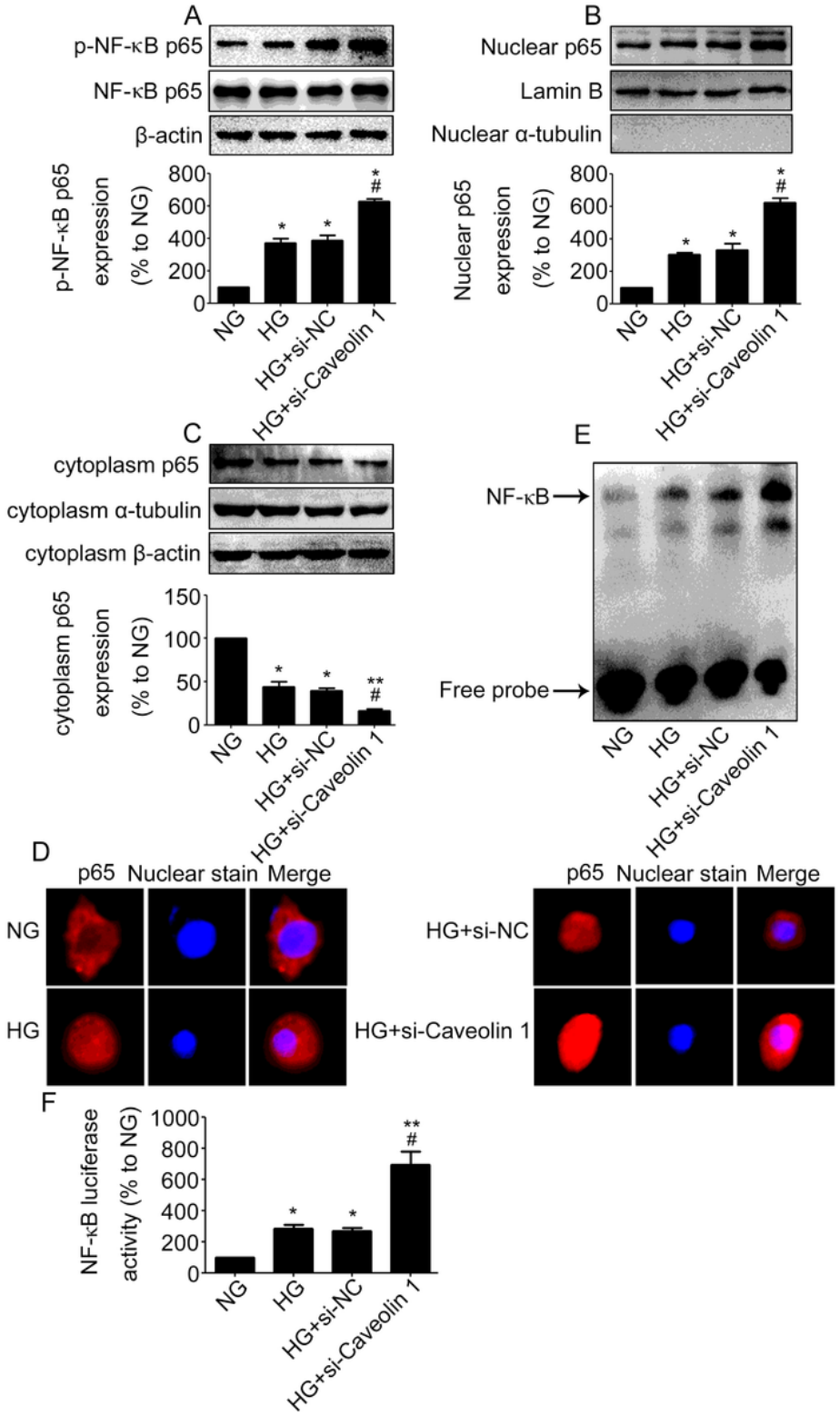

Figure 5

Caveolin 1 knockdown activates NF-κB signaling and enhances the DNA-binding and transcriptional activities of NF-κB. Western blotting of HG-exposed, Caveolin 1 knockdown H9C2 cardiomyocytes to examine: phosphorylation of NF-κB p65 and total NF-κB p65 (A); nuclear p65 (B), and cytoplasmic p65 (C). *P < 0.05, **P 0.01 vs NG, #P < 0.05 vs HG. (D) Immunofluorescence staining for the subcellular distribution of p65. Original magnification, ×630. The DNA-binding (E) and transcriptional activity (F) of

NF-κB were assessed using EMSA and luciferase reporter assay. *P < 0.05, **P < 0.01 vs NG, #P < 0.05 vs HG. All experiments were conducted at least three times and similar results were obtained each time.

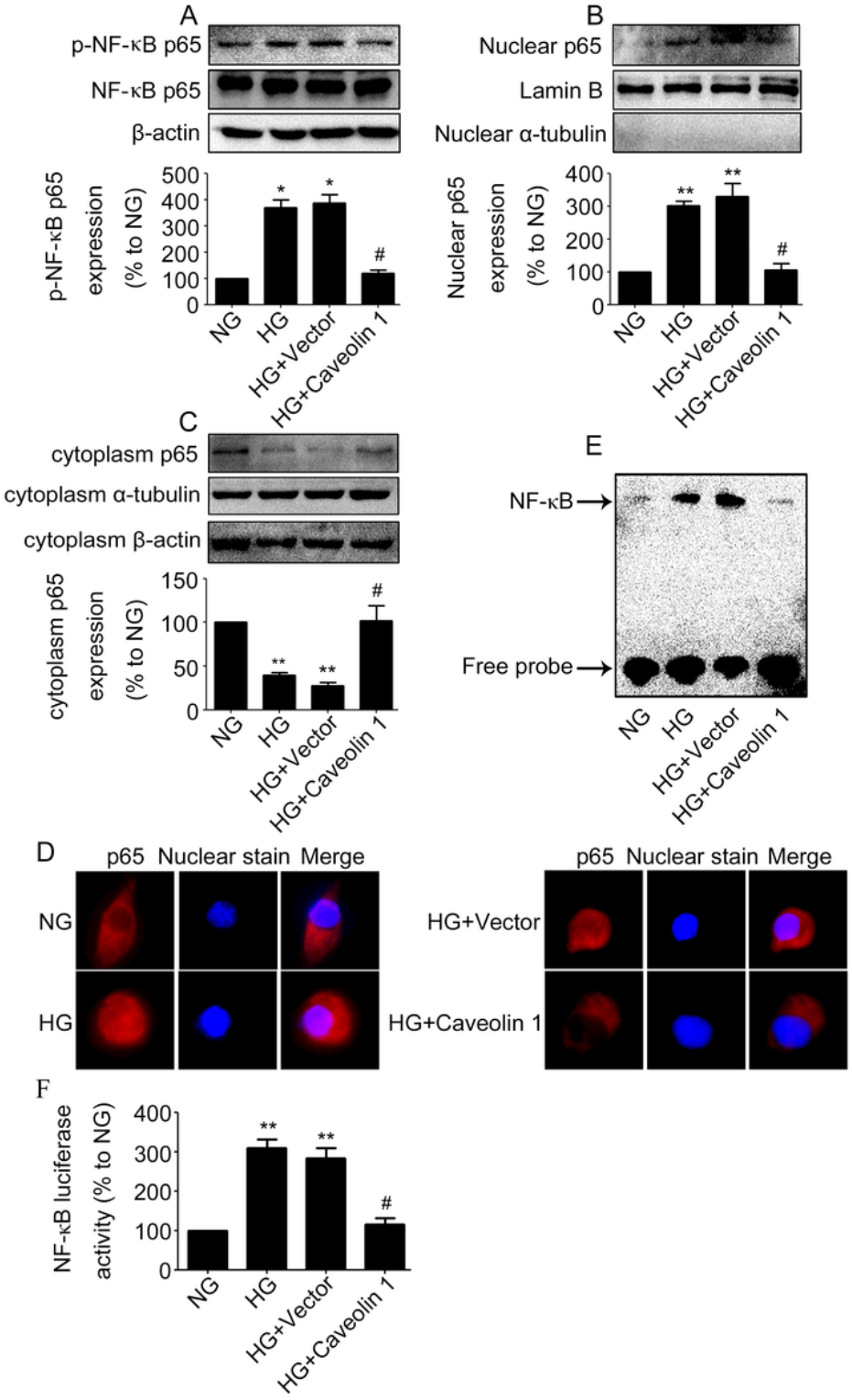

Figure 6

Caveolin 1 overexpression inhibits NF-κB signaling activation, and the DNA-binding and transcriptional activities of NF-κB. The phosphorylation and total NF-κB p65 (A), nuclear (B) and cytoplasm content (C) of p65 levels were detected by western blotting in HG-induction H9C2 cardiomyocytes transfected with

Caveolin 1 plasmid. *P < 0.05, **P < 0.01 vs NG, #P < 0.05 vs HG. (D) Immunofluorescence staining demonstrated the subcellular distribution of p65. Original magnification, ×630. The DNA-binding (E) and transcriptional activities (F) of NF-κB were obtained by EMSA and luciferase reporter assays. **P < 0.01 vs NG, #P < 0.05 vs HG. All experiments were performed at least three times with similar results.